PROCEEDINGS OF SCIENCE

Review of muon g-2: lattice, dispersive, and data driven results

Finn M. Stokes* for the BMW collaboration

Special Research Centre for the Subatomic Structure of Matter, Department of Physics, University of Adelaide, Kaurna Country, South Australia 5005, Australia

Jülich Supercomputing Centre, Institute for Advanced Simulation, Forschungszentrum Jülich, Jülich D-52425, Germany

E-mail: finn.stokes@adelaide.edu.au

Almost twenty years ago, physicists at Brookhaven National Laboratory measured the magnetic moment of the muon with a remarkable precision of 0.54 parts per million. Since that time, the reference Standard Model prediction for this quantity has exhibited a persistent discrepancy with experiment of more than three sigma. This raises the tantalising possibility of undiscovered forces or elementary particles.

The attention of the world was drawn to this discrepancy in 2021 when physicists at Fermilab presented the first results of a new experimental measurement, brilliantly confirming Brookhaven's measurement and bringing the discrepancy to a near discovery level of 4.2 sigma. This discrepancy was further enhanced to 5.1 sigma in 2023 with Fermilab's latest result, which reduces the measurement uncertainty by a factor of 2. However, in the meantime, new tensions have emerged between different determinations of the hadronic vacuum polarisation (HVP) contribution to the theoretical result.

In this contribution, I review the current status of theoretical determinations of the muon anomalous magnetic moment in the context of the latest experimental results. I will particularly focus on our evolving understanding of the HVP, and what this means for the possibility of new physics in this longstanding discrepancy.

The XVIth Quark Confinement and the Hadron Spectrum Conference (QCHSC24)
19-24 August 2024
Cairns Convention Centre, Cairns, Queensland, Australia

*Speaker

PoS(QCHSC24)005

Contents

1. Overview

The magnetic moment of the muon presents a longstanding discrepancy between the Standard Model of particle physics and experimental measurements. Since it was precisely measured at Brookhaven National Laboratory in 2006 [1], ongoing theoretical efforts to compute it show a persistent discrepancy with the measurement [2]. Since the most recent experimental update from the Fermi National Accelerator Laboratory in 2023 [3], the White Paper theory consensus [2] disagrees with the experimental result by more than five sigma, as shown in Figure 1. This should be sufficient evidence for a discovery, however in the meantime several new results call in to question the accuracy of the white paper result.

First, in 2021 the Budapest-Marseille-Wuppertal (BMW) collaboration published a significant update to the theoretical prediction [4] which resolved the tension between the Standard Model and experiment. By combining cutting-edge numerical techniques and world-class supercomputing resources this study provided a sub-percent ab-initio calculation of the main hadronic contribution to the magnetic moment—the hadronic vacuum polarisation (HVP). However, while resolving the tension between the theoretical prediction and the experimental measurements of the magnetic moment, this result created a new tension, this time between two Standard Model determinations of the HVP, as seen in Figure 1. A 2024 update to this result [5] reduced the uncertainties and brought the theory value even closer to the experiment.

Subsequently, a new result from the CMD-3 collaboration [6] and a re-analysis of Tau decay data [7, 8] provided significantly different values for key experimental inputs into the hadronic part of the White Paper theory consensus. This situation is shown in the lower part of Figure 1. It is evident that the status of these experimental inputs to the HVP is much less clear now than it was at the time of the White Paper's publication, and the White Paper result is currently being reassessed.

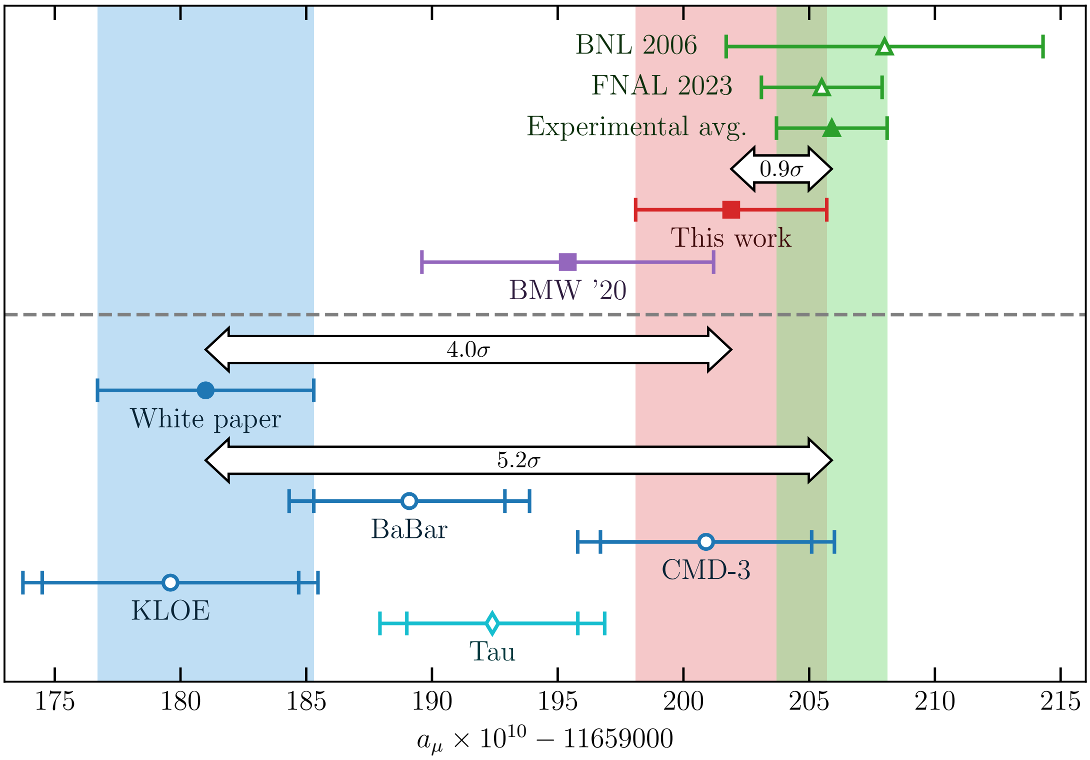

Figure 1: Comparison of standard-model predictions for the muon anomalous magnetic moment with its measured value. The panel above the dashed horizontal line shows a comparison of the world-average measurement of a_μ [3] denoted by a green band, with the standard-model prediction obtained by the BMW collaboration, denoted by the red band. The latter is obtained by adding the value of $a_\mu^{\text{LO-HVP}}$ computed in Ref. [5] to the results for all the other contributions summarised in Ref. [2]. The earlier BMW result from Ref. [4] is also plotted, in purple. The panel below the line shows the predictions for $a_\mu^{\text{LO-HVP}}$ obtained in the data-driven approach of Ref. [2] using the most precise measurements of the two-pion spectrum in electron-positron annihilation and τ-decay experiments [9]. These correspond to BaBar [10, 11], KLOE [12–15] and CMD-3 [6] for e^+e^- annihilation and Tau for τ decays [7, 8]. The blue band shows the muon $g-2$ Theory Initiative combination of the data-driven results [2] (White paper), obtained prior to the publication of the CMD-3 measurement. That combination is currently being reassessed.

2. Anomalous magnetic moment

The specific quantity that shows this discrepancy is the anomalous magnetic moment, which measures the quantum loop corrections to the magnetic moment. It is defined in terms of the g factor of the magnetic moment

$$\vec{\mu} = g\left(\frac{q}{2m}\right)\vec{S}, \tag{1}$$

where q is the charge, m is the mass, $\vec{S}$ is the spin, and g is the g factor. The anomalous magnetic moment is the relative deviation of g from its tree-level value of 2

$$a = \frac{g-2}{2}. \tag{2}$$

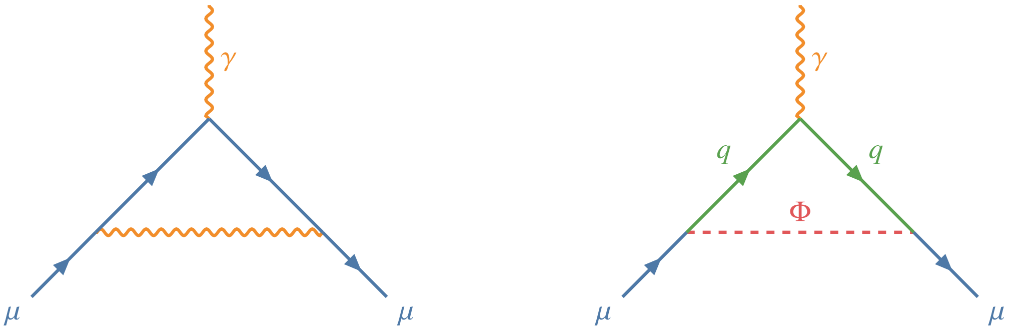

(a) The leading contribution, corresponding to a single virtual photon dressing the vertex

(b) An example of a potential new physics contribution coming from a scalar leptoquark (Φ)

Figure 2: Two different loop diagrams that could contribute to the anomalous magnetic moment of the muon. In both examples, a virtual particle dresses the interaction vertex with the external magnetic field.

The leading contribution to the anomalous magnetic moment comes from the loop arising from a single virtual photon dressing the magnetic interaction vertex as shown in Figure 2a. Higher order contributions come from dressing with weak bosons and/or more loops. Since the anomalous magnetic moment entirely comes from loop diagrams, it is sensitive to many types of BSM physics that could enter into the loop, for example a scalar leptoquark as shown in Figure 2b. This makes the anomalous magnetic moment a powerful probe for new physics, which is why the observed discrepancy is of great interest.

This anomalous magnetic moment is directly measured in the Brookhaven and Fermilab experiments, by injecting a polarised beam of muons into a large magnetic storage ring and observing the rate at which the muons decay. As the muon cycles around the ring, its magnetic moment precesses with a very similar frequency. The difference between the two frequencies is directly related to the anomalous magnetic moment. It can be observed as a modulation of the rate of decay of the muons as the momentum and magnetic moment come in and out of alignment. This is how the experimental results (green triangles) in Figure 1 were obtained.

3. Standard Model predictions

In the Standard Model, the anomalous magnetic moment of the muon is dominated by electromagnetic contributions, which make up 99.994% of the total value. These have been computed in

Contribution	Value		
$a_\mu^{QED} \times 10^{10}$	11 658 471.8931	±	0.0104
$a_\mu^{EW} \times 10^{10}$	15.36	±	0.10
$a_\mu^{HVP} \times 10^{10}$	684.5	±	4.0
$a_\mu^{HLbL} \times 10^{10}$	9.2	±	1.8
$a_\mu \times 10^{10}$	11 659 208.9	±	6.3

Table 1: Individual contributions to the standard model theory consensus from Ref. [2].

perturbation theory to five loops [16, 17], providing a precision of better than one part in a billion, as shown in the first row of Table 1. At this extreme level of precision, the tiny contributions from the other forces need to be precisely determined.

The electroweak contributions, including the effect of the Higgs boson, are heavily suppressed by the masses of the W, Z, and Higgs bosons. Consequentially, they only contribute approximately 0.001% of the total value. These contributions have also been computed in perturbation theory, to two loops [18, 19]. This provides a precision of better than 0.7%, which is more than enough for this tiny contribution, as seen in the second row of Table 1.

The remaining contributions come from the strong force, and are driven by two main effects—the hadronic vacuum polarisation (HVP), and the hadronic light by light scattering (HLbL), shown in Figure 3. These effects contribute approximately 0.006% and 0.0001% of the total value, but together they dominate the uncertainty of the final result, as seen on rows three and four of Table 1. This is because these hadronic effects are fundamentally non-perturbative, and we cannot obtain their contributions through perturbation theory. Instead we must turn to another approach to obtain these values. Two main approaches are currently viable, either a data-driven approach using experimental data from electron-positron colliders [20–23], or an ab-initio computational calculation using lattice QCD [4, 24–27].

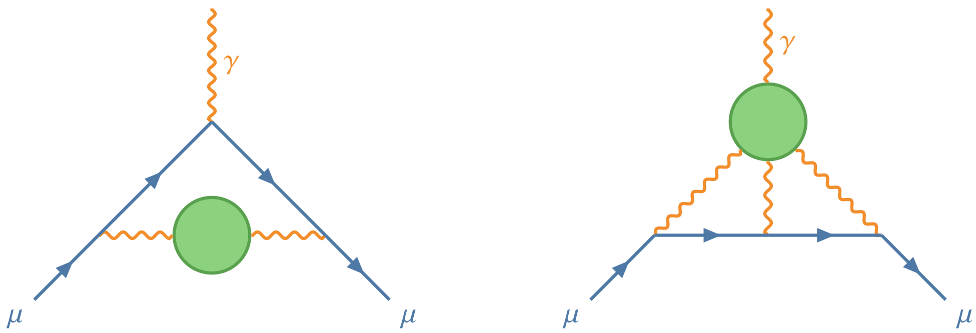

(a) The hadronic vacuum polarisation (HVP) **(b)** The hadronic light-by-light scattering (HLbL)

Figure 3: The major hadronic contributions to the muon magnetic moment. The green blobs encapsulate complicated non-perturbative interactions between quarks and gluons, coupled to the muon through electromagnetic interactions with the quarks.

4. Hadronic Vacuum Polarisation

4.1 Data-driven evaluations

The most common approach to a data-driven calculation of the HVP is to use experimental data on the production of hadronic final states at electron positron colliders. The largest contributions to this experimental dataset come from the BaBar [10, 11] and KLOE [12–15] experiments. Additional contributions the dominant contribution come from CMD2 [28–31], SND [32], and BESIII [33]. Using the optical theorem, this hadronic production data can be related to the process by which a virtual photon mixes with hadronic intermediate states. This mixing is exactly the hadronic vacuum polarisation.

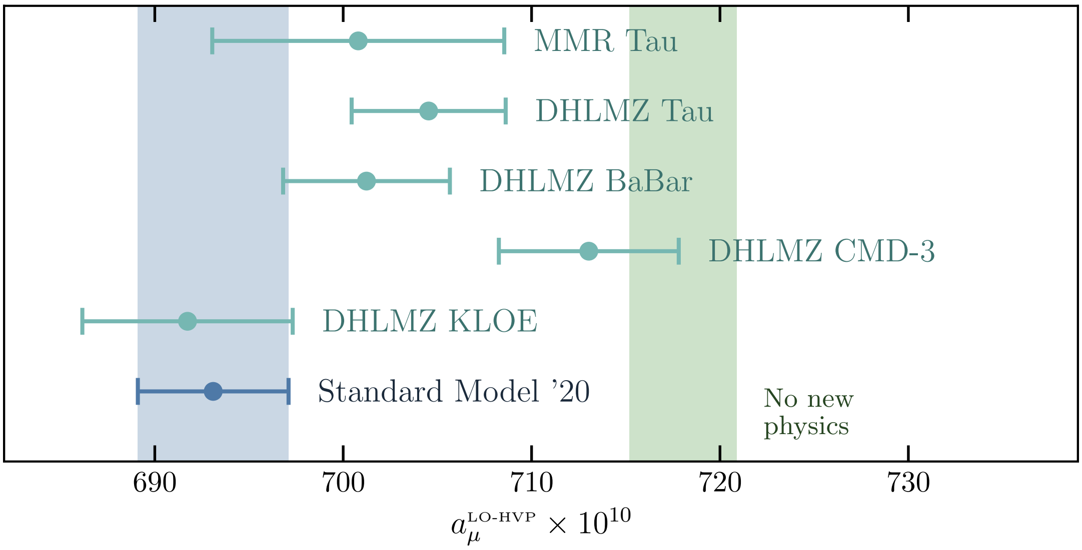

Figure 4: A comparison of data-driven results for the HVP with two-pion production data restricted to specific experimental data sets [9], including results from Tau decays [9, 38]. The scatter of the individual results spans the entire range between the Standard Model consensus [2], and the value required for consistency with the latest experimental average [3], represented by the two shaded bands.

The benchmark Standard Model result for the HVP shown in Table 1 comes from this approach. It is a conservative merging [2] of three different calculations: from KNT [34], DHMZ [35], and CHHKS [22, 23]. It is this combination that is used in the Standard Model consensus that is in 5σ tension with the latest experimental average.

At the time of these calculations, it was known that there were tensions between the BaBar and KLOE experimental results for the production of two pions in the region of the ρ resonance. Efforts were made to quantify these tensions and take them into account in the final uncertainty of the result. Since then, a new result from the CMD-3 experiment [6, 36] is in even stronger tension with the other results, suggesting that this uncertainty was underestimated in the Standard Model consensus. In addition, the BaBar collaboration has raised potential issues with the PHOKARA Monte-Carlo simulations that were used to calibrate many of the experiments, and highlighted how these issues have the potential to significantly effect some of the results, particularly from KLOE and BESIII [37]. This has motivated a re-evaluation of the experimental data entering into the data-driven evaluations, and a revisiting of additional data from tau decays that was previously excluded due to concerns about uncertainties associated with isospin-breaking effects [9].

Figure 4 shows the effect of restricting the input data for the data-driven analysis to specific experiments. The scatter of the individual results spans the entire range between the Standard Model consensus and the latest experimental average. As such, it is hard to say much about the discrepancy using only data-driven calculations, and much work will be needed to quantify and address these tensions in future. An independent approach that is free from these discrepancies is highly desirable.

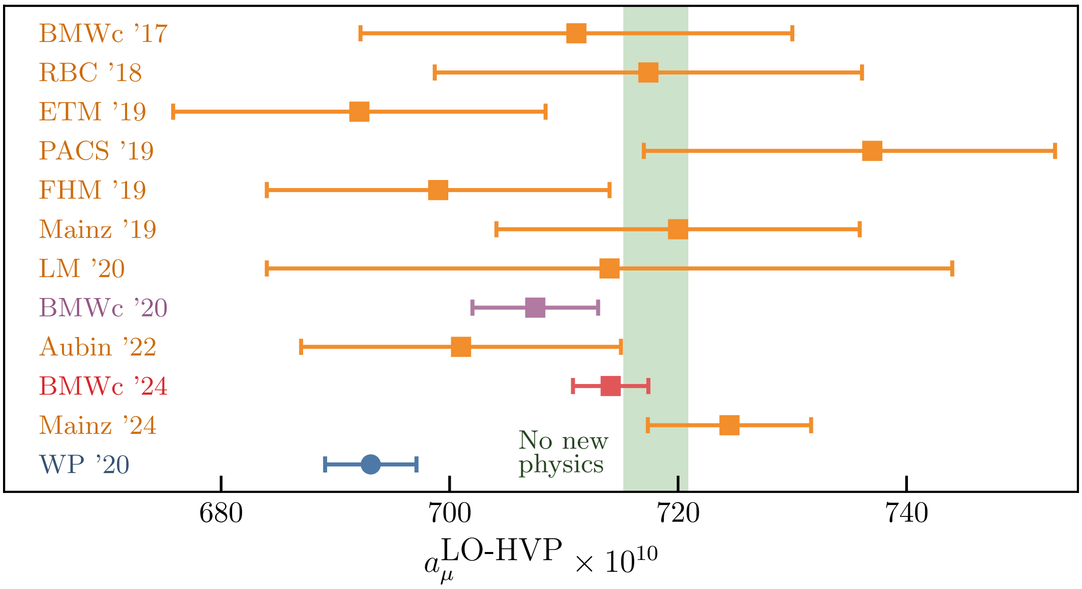

Figure 5: Comparison of lattice values for the leading HVP contribution to the muon magnetic moment. The blue circle is the Standard Model consensus from the White Paper [2], and the squares are lattice results. The older lattice results [40–47] are consistent with both the Standard Model consensus and the experimental measurement. The three most precise points (from BMW [4, 5] and Mainz [24]) agree with the experimental measurement but not the Standard Model consensus.

4.2 Lattice QCD evaluations

Instead of relying on experimental data to obtain the hadronic vacuum polarisation, we can take the QCD+QED Lagrangian and perform an ab-initio calculation to obtain it directly from the underlying theory. However, since low-energy QCD is not amenable to perturbation theory, we need a non-perturbative approach. Lattice QCD is just such an approach. By formulating the Lagrangian on a finite discrete four-dimensional grid or lattice of points (separated by some lattice spacing), we render the problem finite, and allow the path integral to be evaluated by a Monte-Carlo sampling. Performing this sampling requires operating on huge sparse matrices, so these calculations are done on supercomputers.

In order to connect these simulations to experimental reality, we need to fix the parameters of the theory to match nature. The required parameters are the scale of the theory, the masses of the quarks, and the electromagnetic coupling. This is generally done by matching a set of physical observables to their experimental values.

The HVP contribution to the magnetic moment is evaluated using the so-called time-momentum representation [39], whereby it is computed as the integral of a smooth integrand over Euclidean time.

Until 2020, the uncertainties on the HVP from such lattice calculations were consistently larger than those from data-driven determinations, and they were mostly consistent within errors with both the data-driven results and the experimental measurements. As such they were not able to provide

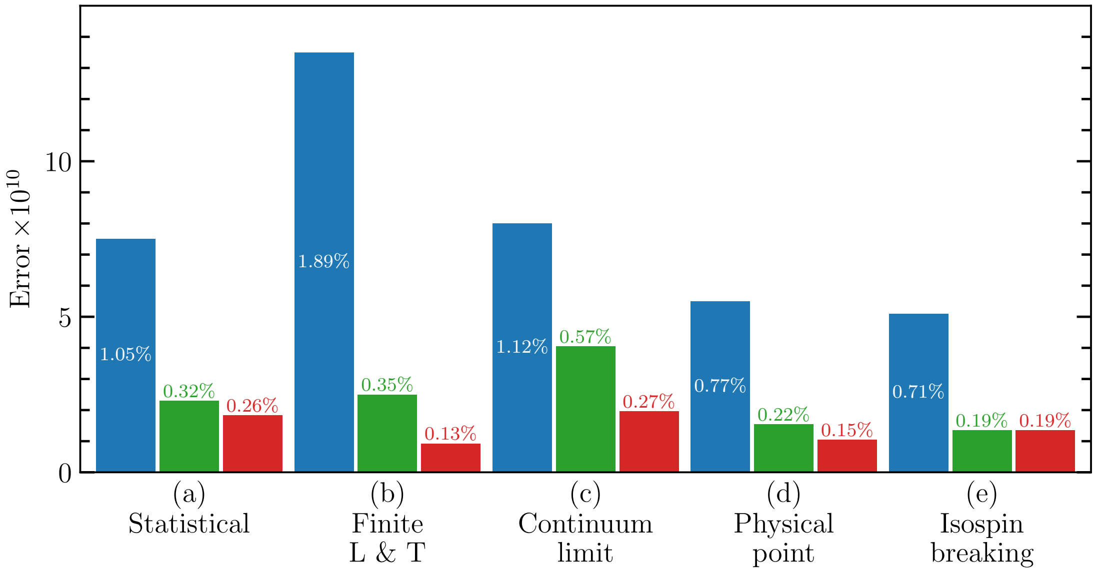

Figure 6: Main uncertainties and their reduction in the BMW collaboration's successive lattice calculations of $a_\mu^{\text{LO-HVP}}$. Their sources are labelled (a-e) in the text and are given a short descriptive title below the bars in the plot. Their approximate size relative to the total LO-HVP contribution obtained in the present work is also shown. The blue bars on the left of each group correspond to the 2017 BMW result [48], the green ones in the middle to the 2020 findings [4], and the red ones on the latest BMW preprint [5].

any insight into the discrepancy. However, in 2020 the BMW collaboration published the first sub-percent lattice determination [4]. This result had errors comparable to the data-driven calculations, but dramatically reduced the tensions with the experimental measurement. Since then, an update from BMW [5] improved the precision even further, and an independent calculation from Mainz [24] confirmed the result, albeit with somewhat larger uncertainty. This can be seen in Figure 5.

The BMW collaboration's 2020 publication was a 3.4× increase in precision compared to our previous work [40], and the 2024 update was a further 1.7× improvement. Many upgrades were required to reach this extreme level of precision, and were made possible thanks to extensive work by many groups around the world in proposing and refining the techniques required.

Figure 6 summarises the five main sources of uncertainty in these lattice QCD calculations, and how they were improved across the three BMW publications to reach the current level of precision. These sources of uncertainty are:

a the statistical Monte-Carlo sampling of the path integral;

b the effects of constraining the simulation to a box of finite size;

c uncertainties in the continuum extrapolation to a lattice spacing of zero; and

d uncertainties on the physical values of the inputs used to set the parameters of the theory;

e isospin-breaking effects from QED and the up-down quark mass difference.

The dominant uncertainties in the 2017 work came from source (b), uncertainties in removing the effect of the 6 fm box in which we perform our simulations. In 2020, these effects were addressed using dedicated large-volume simulations in an 11 fm box. The effects of the finite size of our simulations are exponentially suppressed by the length of the box, so these large-volume simulations see much smaller finite-volume effects. The remaining uncertainties due to residual finite volume effects at 11 fm, and to uncertainties in the 11 fm simulation results were small, and mostly affected the large-Euclidean-time tail of the integrand.

Once this uncertainty was reduced, the other sources became important and had to be reduced to bring the final uncertainty down. Four further improvements in the 2020 work allowed these reductions:

1. Algorithmic improvements [49, 50] allowed increased statistics, improving the statistical and continuum limit uncertainties.
2. New techniques for the exact treatment of infrared modes [51] improved statistical uncertainty.
3. A new scale-setting input (the Ω baryon mass) reduced the uncertainty of the physical point.
4. Calculations of all isospin-breaking effects significantly reduced the associated uncertainty.

In 2024, the analysis was updated with new simulations at a finer lattice spacing, and an overhaul to the analysis procedure. In this work, the Euclidean-time integral was broken up into different windows, and the continuum limit was performed for each window independently. This allowed for a separation of the dominant uncertainties, with different Euclidean times being affected by different sources of uncertainty:

1. The short-distance part has complicated discretisation effects that make the continuum limit challenging, but the statistical errors are small, so it is easy to constrain the form of this extrapolation.
2. The long-distance part has large statistical and finite-size uncertainties.
3. Most of the total value comes from intermediate distances with small statistical errors, and simple well-constrained continuum limits.

Separating out the different distance scales like this significantly improved the lattice uncertainties at short and intermediate distances, but also allowed us to take a novel approach to addressing uncertainties in the long-distance tail beyond 2.8 fm. This region is challenging to compute in lattice QCD, with large statistical uncertainty and finite volume effects, and a strong dependence on the scale of the theory, despite only contributing about 5% of the total value. However, this tail is dominated by energies well below the ρ resonance, a region where the discrepancies that plague the data-driven approach disappear, as seen in Figure 7. By replacing this small part of the integral with a data driven calculation, the finite volume uncertainty is significantly reduced, and the statistical and physical point uncertainties are also improved.

The 2024 calculation from BMW was performed completely blind, with all HVP data multiplied by unknown random numbers before analysis commenced. These blinding factors were only removed once the analysis was finalised and the manuscript was almost complete. This ensured the

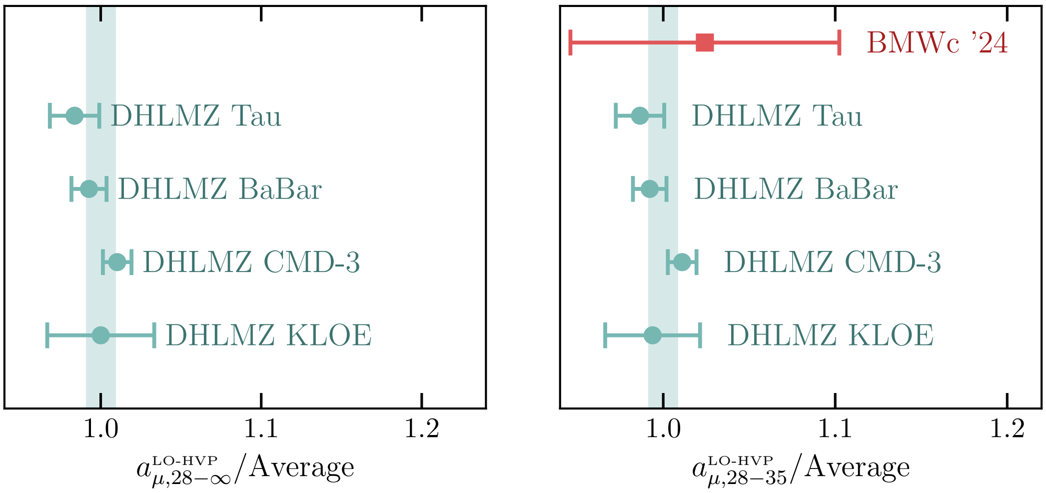

Figure 7: A comparison of relative deviations of data-driven results for the long-distance tail of the HVP with two-pion production data restricted to specific experimental data sets, including results from Tau decays [5]. The shaded bands represent an average of the data-driven points, and all points are relative to the central value of that average. The left panel is the entire tail from 2.8 fm to infinity, and the right panel is a comparison with lattice for the part of the tail from 2.8 fm to 3.5 fm. The scatter of the individual results is consistent with their uncertainties, and the lattice result agrees well, although its errors are larger. The shaded band is a combination of the data-driven points.

result was free from any conscious or unconscious biases from any of the researchers. As seen in Figure 5, this result is in good agreement with the recent lattice result from Mainz [24], and with the experimental measurement.

On the other hand, there is a significant tension between the lattice QCD calculations and the data-driven determinations of the HVP. It is important to understand this discrepancy in order to ascertain whether this is a sign of new physics, or some gap in our understanding of standard model physics.

So where could the discrepancy come from? Some efforts towards answering this question have already been made. In terms of Standard model physics, phenomenological estimates have shown that there is no way for isospin breaking contributions to explain the discrepancy [52]. In terms of new physics, it has been suggested that a GeV scale dark photon could explain not only the discrepancy between the lattice result and the data-driven consensus, but also the discrepancies between the experiments themselves [53]. However, many regions of the parameter space have already been excluded by other experiments, so something more complicated may be needed.

One way to try to narrow down the possibilities is to try to identify the energy ranges that the lattice and data-driven determinations disagree at. To naïvely convert from the Euclidean time integrand computed on the lattice to the energy spectrum that is input to the data-driven calculation requires an inverse Laplace transform. This is an ill-conditioned problem and is not practically solvable with the data we have. Two possible workarounds have been explored:

1. A collaboration between BMW and DMZ has considered what modifications to the data

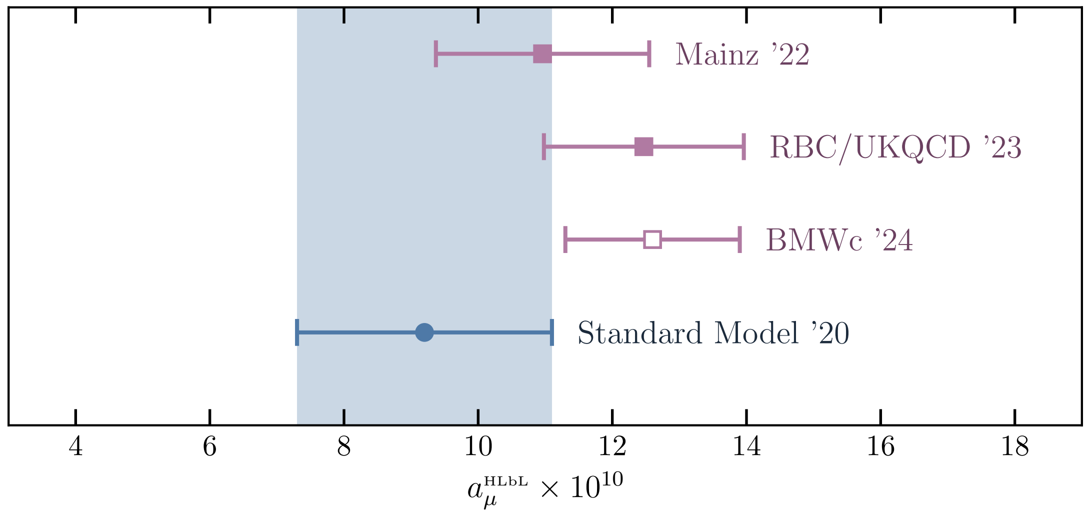

Figure 8: Different determinations of the leading-order hadronic light-by-light contribution, showing lattice results (purple squares) and the consensus data-driven result (blue circle), which are in good agreement. The open square is a lattice result from a preprint by the BMW collaboration.

driven input would give consistency and systematically identified how well they agree with the known data [54].

2. The ETM collaboration have explored the computation of a smeared version of the energy spectrum, which is much better conditioned, and also easy to compute from the experimental data [55].

Both approaches give consistent results, suggesting an enhancement of the spectrum observed at BaBar and KLOE by around 5% in the region of the ρ resonance. This gives an energy spectrum that is similar to what is observed at CMD-3.

Further efforts will be needed to fully understand this discrepancy and to determine the ramifications.

5. Hadronic Light-by Light

Because the HLbL contribution is much smaller than the HVP, it only needs to be determined to a precision of approximately 10% to meet the target precision for the total result, or 30% to surpass the current precision in the HVP.

The data driven calculation of the HLbL is more complicated than the HVP, but the necessary procedure was figured out in 2015 [56]. Utilising a variety of experimental data, with some input from lattice QCD [57] the individual contributions can be computed in a dispersive framework [58–69], obtaining a relative error of 20% [2], which is smaller than the current error from the HVP. This result is shown by the blue circle in Figure 8.

Full ab-initio lattice QCD calculations have also been performed [25–27], obtaining similar uncertainties and consistent values. These are shown as purple squares in Figure 8.

The agreement between different determinations of the HLbL is good, and ongoing efforts are on track to improve the determinations to reach the target precision in the next few years. Overall, HLbL looks to be in a good place.

6. Conclusion

Recent lattice QCD results have surpassed the precision of all other theoretical predictions of the hadronic vacuum polarisation contribution to the muon magnetic moment. When taken together with the latest theory consensus for QED, EW, and HLbL contributions [2], these results show excellent agreement with the latest experimental measurements [3]. This a remarkable success for quantum field theory, bringing together diverse computational tools to include all aspects of the Standard Model in a single calculation that validates the Standard Model to 0.37 ppm.

References

[1] Muon g-2 collaboration, *Final Report of the Muon E821 Anomalous Magnetic Moment Measurement at BNL*, *Phys. Rev. D* **73** (2006) 072003 [hep-ex/0602035].

[2] T. Aoyama et al., *The anomalous magnetic moment of the muon in the Standard Model*, *Phys. Rept.* **887** (2020) 1 [arXiv:2006.04822].

[3] Muon g-2 collaboration, *Measurement of the Positive Muon Anomalous Magnetic Moment to 0.20 ppm*, *Phys. Rev. Lett.* **131** (2023) 161802 [arXiv:2308.06230].

[4] S. Borsanyi et al., *Leading hadronic contribution to the muon magnetic moment from lattice QCD*, *Nature* **593** (2021) 51 [arXiv:2002.12347].

[5] A. Boccaletti et al., *High precision calculation of the hadronic vacuum polarisation contribution to the muon anomaly*, arXiv:2407.10913.

[6] CMD-3 collaboration, *Measurement of the e+e-→π+π- cross section from threshold to 1.2 GeV with the CMD-3 detector*, *Phys. Rev. D* **109** (2024) 112002 [arXiv:2302.08834].

[7] M. Davier, A. Hoecker, G. Lopez Castro, B. Malaescu, X. Mo, G. Toledo Sanchez et al., *The Discrepancy Between tau and e+e- Spectral Functions Revisited and the Consequences for the Muon Magnetic Anomaly*, *Eur. Phys. J. C* **66** (2010) 127 [arXiv:0906.5443].

[8] M. Davier, A. Höcker, B. Malaescu, C.-Z. Yuan and Z. Zhang, *Update of the ALEPH non-strange spectral functions from hadronic τ decays*, *Eur. Phys. J. C* **74** (2014) 2803 [arXiv:1312.1501].

[9] M. Davier, A. Hoecker, A.-M. Lutz, B. Malaescu and Z. Zhang, *Tensions in $e^+e^- \to \pi^+\pi^-(\gamma)$ measurements: the new landscape of data-driven hadronic vacuum polarization predictions for the muon $g-2$*, *Eur. Phys. J. C* **84** (2024) 721 [arXiv:2312.02053].

[10] BaBar collaboration, *Precise measurement of the e+ e- —> pi+ pi- (gamma) cross section with the Initial State Radiation method at BABAR*, *Phys. Rev. Lett.* **103** (2009) 231801 [arXiv:0908.3589].

[11] BaBar collaboration, *Precise Measurement of the $e^+e^- \to \pi^+\pi^-(\gamma)$ Cross Section with the Initial-State Radiation Method at BABAR*, *Phys. Rev. D* **86** (2012) 032013 [arXiv:1205.2228].

[12] KLOE collaboration, *Measurement of $\sigma(e^+e^- \to \pi^+\pi^-\gamma(\gamma))$ and the dipion contribution to the muon anomaly with the KLOE detector*, *Phys. Lett. B* **670** (2009) 285 [arXiv:0809.3950].

[13] KLOE collaboration, *Measurement of $\sigma(e^+e^- \to \pi^+\pi^-)$ from threshold to 0.85 GeV^2 using Initial State Radiation with the KLOE detector*, *Phys. Lett. B* **700** (2011) 102 [arXiv:1006.5313].

[14] KLOE collaboration, *Precision measurement of $\sigma(e^+e^- \to \pi^+\pi^-\gamma)/\sigma(e^+e^- \to \mu^+\mu^-\gamma)$ and determination of the $\pi^+\pi^-$ contribution to the muon anomaly with the KLOE detector*, *Phys. Lett. B* **720** (2013) 336 [arXiv:1212.4524].

[15] KLOE-2 collaboration, *Combination of KLOE $\sigma\big(e^+e^- \to \pi^+\pi^-\gamma(\gamma)\big)$ measurements and determination of $a_\mu^{\pi^+\pi^-}$ in the energy range $0.10 < s < 0.95$ GeV^2*, *JHEP* **03** (2018) 173 [arXiv:1711.03085].

[16] T. Aoyama, T. Kinoshita and M. Nio, *Theory of the Anomalous Magnetic Moment of the Electron*, *Atoms* **7** (2019) 28.

[17] T. Aoyama, M. Hayakawa, T. Kinoshita and M. Nio, *Complete Tenth-Order QED Contribution to the Muon g-2*, *Phys. Rev. Lett.* **109** (2012) 111808 [arXiv:1205.5370].

[18] A. Czarnecki, W.J. Marciano and A. Vainshtein, *Refinements in electroweak contributions to the muon anomalous magnetic moment*, *Phys. Rev. D* **67** (2003) 073006 [hep-ph/0212229].

[19] C. Gnendiger, D. Stöckinger and H. Stöckinger-Kim, *The electroweak contributions to $(g-2)_\mu$ after the Higgs boson mass measurement*, *Phys. Rev. D* **88** (2013) 053005 [arXiv:1306.5546].

[20] M. Davier, A. Hoecker, B. Malaescu and Z. Zhang, *A new evaluation of the hadronic vacuum polarisation contributions to the muon anomalous magnetic moment and to $\boldsymbol{\alpha}(\mathbf{m_Z^2})$*, *Eur. Phys. J. C* **80** (2020) 241 [arXiv:1908.00921].

[21] A. Keshavarzi, D. Nomura and T. Teubner, *$g-2$ of charged leptons, $\alpha(M_Z^2)$, and the hyperfine splitting of muonium*, *Phys. Rev.* **D101** (2020) 014029 [arXiv:1911.00367].

[22] G. Colangelo, M. Hoferichter and P. Stoffer, *Two-pion contribution to hadronic vacuum polarization*, *JHEP* **02** (2019) 006 [arXiv:1810.00007].

[23] M. Hoferichter, B.-L. Hoid and B. Kubis, *Three-pion contribution to hadronic vacuum polarization*, *JHEP* **08** (2019) 137 [arXiv:1907.01556].

[24] D. Djukanovic, G. von Hippel, S. Kuberski, H.B. Meyer, N. Miller, K. Ottnad et al., *The hadronic vacuum polarization contribution to the muon $g-2$ at long distances*, arXiv:2411.07969.

[25] E.-H. Chao, R.J. Hudspith, A. Gérardin, J.R. Green and H.B. Meyer, *The charm-quark contribution to light-by-light scattering in the muon $(g-2)$ from lattice QCD*, *Eur. Phys. J. C* **82** (2022) 664 [arXiv:2204.08844].

[26] RBC, UKQCD collaboration, *Hadronic light-by-light contribution to the muon anomaly from lattice QCD with infinite volume QED at physical pion mass*, *Phys. Rev. D* **111** (2025) 014501 [arXiv:2304.04423].

[27] Z. Fodor, A. Gerardin, L. Lellouch, K.K. Szabo, B.C. Toth and C. Zimmermann, *Hadronic light-by-light scattering contribution to the anomalous magnetic moment of the muon at the physical pion mass*, arXiv:2411.11719.

[28] CMD-2 collaboration, *Reanalysis of hadronic cross-section measurements at CMD-2*, *Phys. Lett. B* **578** (2004) 285 [hep-ex/0308008].

[29] CMD-2 collaboration, *Measurement of the pion form-factor in the range 1.04-GeV to 1.38-GeV with the CMD-2 detector*, *JETP Lett.* **82** (2005) 743 [hep-ex/0603021].

[30] V.M. Aul'chenko et al., *Measurement of the e+ e- —> pi+ pi- cross section with the CMD-2 detector in the 370 - 520-MeV c.m. energy range*, *JETP Lett.* **84** (2006) 413 [hep-ex/0610016].

[31] CMD-2 collaboration, *High-statistics measurement of the pion form factor in the rho-meson energy range with the CMD-2 detector*, *Phys. Lett. B* **648** (2007) 28 [hep-ex/0610021].

[32] M.N. Achasov et al., *Update of the e+ e- —> pi+ pi- cross-section measured by SND detector in the energy region 400-MeV < s**(1/2) < file1000-MeV*, *J. Exp. Theor. Phys.* **103** (2006) 380 [hep-ex/0605013].

[33] BESIII collaboration, *Measurement of the $e^+e^- \to \pi^+\pi^-$ cross section between 600 and 900 MeV using initial state radiation*, *Phys. Lett. B* **753** (2016) 629 [arXiv:1507.08188].

[34] A. Keshavarzi, D. Nomura and T. Teubner, *Muon $g-2$ and $\alpha(M_Z^2)$: a new data-based analysis*, *Phys. Rev.* **D97** (2018) 114025 [arXiv:1802.02995].

[35] M. Davier, A. Hoecker, B. Malaescu and Z. Zhang, *Reevaluation of the hadronic vacuum polarisation contributions to the Standard Model predictions of the muon $g-2$ and $\alpha(M_Z^2)$ using newest hadronic cross-section data*, *Eur. Phys. J.* **C77** (2017) 827 [arXiv:1706.09436].

[36] CMD-3 collaboration, *Measurement of the Pion Form Factor with CMD-3 Detector and its Implication to the Hadronic Contribution to Muon (g-2)*, *Phys. Rev. Lett.* **132** (2024) 231903 [arXiv:2309.12910].

[37] BaBar collaboration, *Measurement of additional radiation in the initial-state-radiation processes e+e-→μ+μ-γ and e+e-→π+π-γ at BABAR*, *Phys. Rev. D* **108** (2023) L111103 [arXiv:2308.05233].

[38] P. Masjuan, A. Miranda and P. Roig, *τ data-driven evaluation of Euclidean windows for the hadronic vacuum polarization*, *Phys. Lett. B* **850** (2024) 138492 [arXiv:2305.20005].

[39] D. Bernecker and H.B. Meyer, *Vector Correlators in Lattice QCD: Methods and applications*, *Eur. Phys. J.* **A47** (2011) 148 [arXiv:1107.4388].

[40] Budapest-Marseille-Wuppertal collaboration, *Hadronic vacuum polarization contribution to the anomalous magnetic moments of leptons from first principles*, *Phys. Rev. Lett.* **121** (2018) 022002 [arXiv:1711.04980].

[41] RBC, UKQCD collaboration, *Calculation of the hadronic vacuum polarization contribution to the muon anomalous magnetic moment*, *Phys. Rev. Lett.* **121** (2018) 022003 [arXiv:1801.07224].

[42] D. Giusti and S. Simula, *Lepton anomalous magnetic moments in Lattice QCD+QED*, *PoS* **LATTICE2019** (2019) 104 [arXiv:1910.03874].

[43] PACS collaboration, *Hadronic vacuum polarization contribution to the muon $g-2$ with 2+1 flavor lattice QCD on a larger than (10 fm)^4 lattice at the physical point*, *Phys. Rev. D* **100** (2019) 034517 [arXiv:1902.00885].

[44] Fermilab Lattice, LATTICE-HPQCD, MILC collaboration, *Hadronic-vacuum-polarization contribution to the muon's anomalous magnetic moment from four-flavor lattice QCD*, *Phys. Rev. D* **101** (2020) 034512 [arXiv:1902.04223].

[45] A. Gerardin, M. Ce, G. von Hippel, B. Horz, H.B. Meyer, D. Mohler et al., *The leading hadronic contribution to $(g-2)_\mu$ from lattice QCD with $N_f = 2+1$ flavours of O(a) improved Wilson quarks*, *Phys. Rev.* **D100** (2019) 014510 [arXiv:1904.03120].

[46] C. Lehner and A.S. Meyer, *Consistency of hadronic vacuum polarization between lattice QCD and the R-ratio*, *Phys. Rev. D* **101** (2020) 074515 [arXiv:2003.04177].

[47] C. Aubin, T. Blum, M. Golterman and S. Peris, *Muon anomalous magnetic moment with staggered fermions: Is the lattice spacing small enough?*, *Phys. Rev. D* **106** (2022) 054503 [arXiv:2204.12256].

[48] Budapest-Marseille-Wuppertal collaboration, *Hadronic vacuum polarization contribution to the anomalous magnetic moments of leptons from first principles*, *Phys. Rev. Lett.* **121** (2018) 022002 [arXiv:1711.04980].

[49] G.S. Bali, S. Collins and A. Schafer, *Effective noise reduction techniques for disconnected loops in Lattice QCD*, *Comput. Phys. Commun.* **181** (2010) 1570 [arXiv:0910.3970].

[50] T. Blum, T. Izubuchi and E. Shintani, *New class of variance-reduction techniques using lattice symmetries*, *Phys. Rev.* **D88** (2013) 094503 [arXiv:1208.4349].

[51] H. Neff, N. Eicker, T. Lippert, J.W. Negele and K. Schilling, *On the low fermionic eigenmode dominance in QCD on the lattice*, *Phys. Rev.* **D64** (2001) 114509 [hep-lat/0106016].

[52] M. Hoferichter, G. Colangelo, B.-L. Hoid, B. Kubis, J.R. de Elvira, D. Schuh et al., *Phenomenological Estimate of Isospin Breaking in Hadronic Vacuum Polarization*, *Phys. Rev. Lett.* **131** (2023) 161905 [arXiv:2307.02532].

[53] L. Darmé, G. Grilli di Cortona and E. Nardi, *Indirect new physics effects on σhad confront the (g-2)μ window discrepancies and the CMD-3 result*, *Phys. Rev. D* **108** (2023) 095056 [arXiv:2212.03877].

[54] M. Davier, Z. Fodor, A. Gerardin, L. Lellouch, B. Malaescu, F.M. Stokes et al., *Hadronic vacuum polarization: Comparing lattice QCD and data-driven results in systematically improvable ways*, *Phys. Rev. D* **109** (2024) 076019 [arXiv:2308.04221].

[55] A. De Santis et al., *Lattice calculation of the R-ratio smeared with Gaussian kernels*, *PoS* **LATTICE2022** (2023) 307 [arXiv:2212.12493].

[56] G. Colangelo, M. Hoferichter, M. Procura and P. Stoffer, *Dispersion relation for hadronic light-by-light scattering: theoretical foundations*, *JHEP* **09** (2015) 074 [arXiv:1506.01386].

[57] A. Gérardin, H.B. Meyer and A. Nyffeler, *Lattice calculation of the pion transition form factor with $N_f = 2 + 1$ Wilson quarks*, *Phys. Rev. D* **100** (2019) 034520 [arXiv:1903.09471].

[58] K. Melnikov and A. Vainshtein, *Hadronic light-by-light scattering contribution to the muon anomalous magnetic moment revisited*, *Phys. Rev. D* **70** (2004) 113006 [hep-ph/0312226].

[59] P. Masjuan and P. Sanchez-Puertas, *Pseudoscalar-pole contribution to the $(g_\mu - 2)$: a rational approach*, *Phys. Rev. D* **95** (2017) 054026 [arXiv:1701.05829].

[60] G. Colangelo, M. Hoferichter, M. Procura and P. Stoffer, *Dispersion relation for hadronic light-by-light scattering: two-pion contributions*, *JHEP* **04** (2017) 161 [arXiv:1702.07347].

[61] M. Hoferichter, B.-L. Hoid, B. Kubis, S. Leupold and S.P. Schneider, *Dispersion relation for hadronic light-by-light scattering: pion pole*, *JHEP* **10** (2018) 141 [arXiv:1808.04823].

[62] J. Bijnens, N. Hermansson-Truedsson and A. Rodríguez-Sánchez, *Short-distance constraints for the HLbL contribution to the muon anomalous magnetic moment*, *Phys. Lett. B* **798** (2019) 134994 [arXiv:1908.03331].

[63] G. Colangelo, F. Hagelstein, M. Hoferichter, L. Laub and P. Stoffer, *Longitudinal short-distance constraints for the hadronic light-by-light contribution to $(g-2)_\mu$ with large-N_c Regge models*, *JHEP* **03** (2020) 101 [arXiv:1910.13432].

[64] V. Pauk and M. Vanderhaeghen, *Single meson contributions to the muon's anomalous magnetic moment*, *Eur. Phys. J. C* **74** (2014) 3008 [arXiv:1401.0832].

[65] I. Danilkin and M. Vanderhaeghen, *Light-by-light scattering sum rules in light of new data*, *Phys. Rev. D* **95** (2017) 014019 [arXiv:1611.04646].

[66] F. Jegerlehner, *The Anomalous Magnetic Moment of the Muon*, *Springer Tracts Mod. Phys.* **274** (2017) pp.1.

[67] M. Knecht, S. Narison, A. Rabemananjara and D. Rabetiarivony, *Scalar meson contributions to a μ from hadronic light-by-light scattering*, *Phys. Lett. B* **787** (2018) 111 [arXiv:1808.03848].

[68] G. Eichmann, C.S. Fischer and R. Williams, *Kaon-box contribution to the anomalous magnetic moment of the muon*, *Phys. Rev. D* **101** (2020) 054015 [arXiv:1910.06795].

[69] P. Roig and P. Sanchez-Puertas, *Axial-vector exchange contribution to the hadronic light-by-light piece of the muon anomalous magnetic moment*, *Phys. Rev. D* **101** (2020) 074019 [arXiv:1910.02881].